Sage Geosystems Proprietary sCO2 Turbine Flow Loop Testing

Jordan Nielson and Nathan Weiss

Southwest Research Institute and Sage Geosystems

Keywords

Supercritical CO2 (sCO2), sCO2 Turbine, sCO2 Power Cycle, Flow Loop

ABSTRACT

Sage Geosystems will present the status of the testing of their full-scale 3MWe (electric) prototype supercritical CO2 (sCO2) turbine that has been modeled, designed, and built in a partnership with Southwest Research Institute (SwRI). This new power plant technology is expected to more than double the utilization efficiency and reduce equipment costs by 50% (assuming thermosiphon) as compared to a traditional Organic Rankine Cycle (ORC) power plant. Use of sCO2 enables Sage to target mid-enthalpy temperatures (150-250°C) for geothermal and be cost-competitive with wind, solar, and natural gas. Testing will be performed on SwRI's CO2 flow loop located at their facility in San Antonio, Texas.

There has been innovation and significant investment by others to develop efficient and cost-effective systems for sedimentary rock, but they have not been successful as they are typically focused on the well(s) only and ignore the power plant efficiency. Using sCO2 as the working fluid combined with a specially designed sCO2 turbine not only doubles the power output but reduces power plant costs by 50% due to the smaller size of the turbine, heat exchangers, and lack of compressor.

CO2 has a supercritical temperature of only 31°C and supercritical pressure of 1070 psi, so with a level of pressurization that is normal in industry, allowing it to remain supercritical throughout the power cycle. Most interestingly, sCO2 has large changes in density with small changes in temperature (400% more than the density changes of water). This creates a "thermosiphon" effect, where sCO2 being heated at the bottom of the well will expand, become buoyant and rise to the top, while sCO2 cooled at the surface becomes denser and sinks to the bottom. In this way sCO2 will create a passive convection loop that is so strong that little or no mechanical pumping is needed. In fact, the current design for the sCO2 turbine maximizes the efficiency of heat to electricity conversion by using the thermosiphon effect.

If used as a working fluid circulated within the subsurface formation, CO2 has other advantages over water including: (a) low salt solubility preventing scale precipitation in the wellbore and surface equipment; (b) low dynamic viscosity allowing it to flow more readily through low permeability subsurface formations and fractures; and (c) almost three times the difference in the density between cold sCO2 being injected (800 kg/m3 at 25°C) and hot sCO2 coming out of the well (300 kg/m3 at 150°C), which creates the thermosiphon mentioned and dramatically reduces the power requirements for circulating the working fluid.

1. Introduction

Geothermal is generally seen as a renewable power production source that is also capable of providing a base load (De Jesus 2016). The three main types of power plants that have been utilized to date for geothermal power production are the flashed steam (resource temperatures of 320°C), flashed steam back pressure (double flash) (200-320°C), and binary (120-190°C) (Eliasson, Thorhallsson, and Steingrímsson 2011). A fourth type, namely a thermosiphon plant, has recently been studied but not yet implemented in practice (Atrens, Gurgenci, and Rudolph 2009). The two flash steam types make up almost all the current geothermal power plants but are location dependent due to the very specific types of geologic resources that are needed. The low temperature resources cause binary plants to suffer from lower cycle efficiencies and high capital costs that make them difficult to be cost competitive with other sources of power (traditional geothermal, fossil fuels, wind and solar).

sCO2 provides many unique advantages over water and other traditional refrigerants. First, the wide swings in density allow for sCO2 to work as thermosiphon (also known as a natural convection cycle). A traditional cycle, such as a Brayton or organic Rankine Cycle (ORC), require the working fluid to be compressed or pumped. Because the critical point of sCO2 is at 31°C (near ambient conditions in most locations), the fluid can have a significant (i.e., three times) reduction in density when going from ambient conditions (20-35°C) to a mid-enthalpy temperature (100-250°C). The fluid, in its dense state, is injected into the well and heated near the bottom and the density reduces. The density of the fluid therefore drives the fluid and creates pressure (Atrens, Gurgenci, and Rudolph 2009; Katcher et al., n.d.). This phenom would therefore drive the power generating equipment, similarly to how the hydrodynamic head of a water dam powers hydro turbines.

sCO2 also benefits from additional flexibility. Although it clearly has advantages as working in a thermosiphon cycle, it also has benefits over traditional ORC technologies when used as a binary cycle as well. Persichilli et al. (Persichilli et al. 2012) explain the benefits of sCO2 when it comes to the hot heat exchanger of a binary cycle. The heat transfer of CO2 occurs in a single phase (supercritical) while ORC and steam-based technologies occur at a phase change. During the phase change, the fluid remains at a constant temperature while heat is transferred. This creates a “pinch” point problem and limits the actual temperature of the boiling fluid. The single-phase heat exchange of the CO2 allows for the “pinch” point to occur on the hot side maximizing the temperature into the turbine inlet.

Another significant advantage of sCO2 is its density. sCO2 has a large density, even when hot and expanded compared to other working fluids. The density allows the size of the turbomachinery and heat exchangers to be reduced, therefore, reducing the overall footprint and cost of a power plant (Persichilli et al. 2012; Sudhoff et al. 2019).

This paper describes the research and development activities for the design and testing of a protype sCO2 turbine for mid-enthalpy geothermal applications.

2. sCO2 Turbine Parameters

At the onset of turbine detailed design, a model was developed in order to quantify the inlet pressures and temperatures of the sCO2 turbine (Nielson, Katcher, and Simkins 2022). The model investigated casing diameters of 9-5/8'', 11-3/4'', 13-5/8'', and 16'' at various reservoir/rock temperatures. The results are shown in Figure 1 with the turbine inlet temperature ranging from 110-160°C and the turbine inlet pressure ranging from 14-16 MPa. The turbine isentropic power varied from 1.5- 5.5 MW.

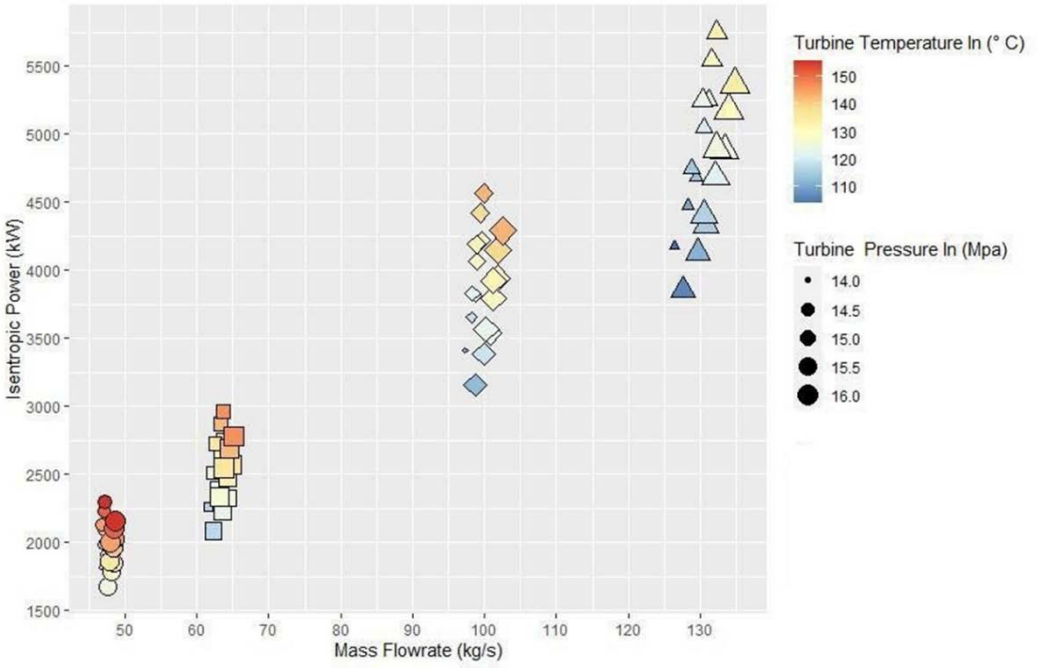

Figure 1. Turbine inlet condition based on various well casing diameters.

The analysis for Figure 1 was performed as an on-design condition only, therefore, a 13-5/8'' casing was further examined for a full year (assuming ambient conditions of south Texas). Figure 2 shows both the turbine power output (assumed 70% isentropic efficiency) and inlet/outlet pressure conditions for the turbine operating over a complete year. The graphs show that the turbine power and pressure will fluctuate due to the swing in ambient conditions. The discontinuity comes from an assumption that the turbine stage will be switched halfway through the year as ambient temperature increases (described more fully later). Therefore, the turbine design needs to be flexible and manage significant changes in pressure conditions.

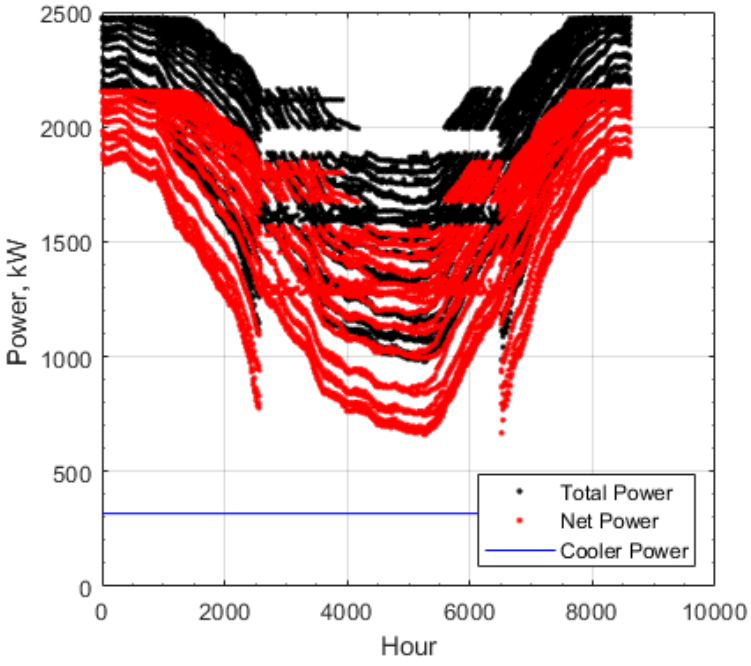

(a)

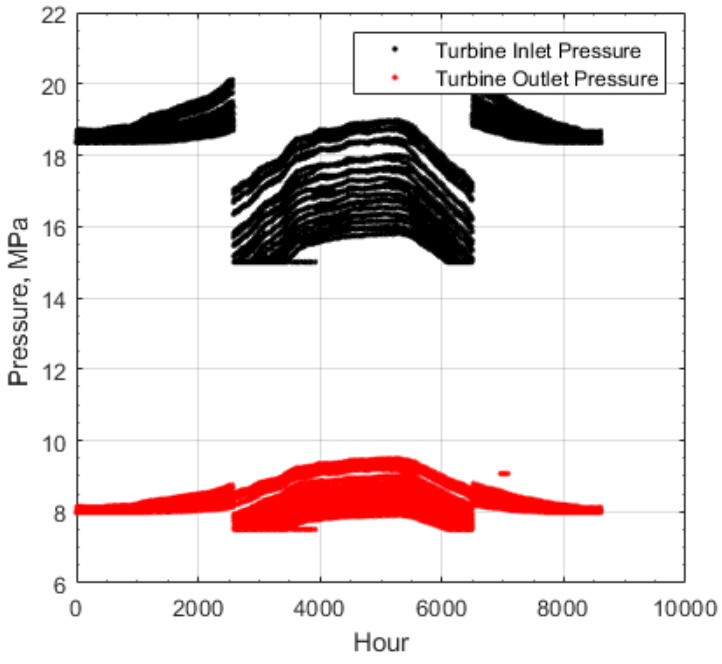

(b)

Figure 2. Annual model for South Texas using dry coolers (a) power output and (b) Turbine inlet and Outlet pressure

The team also performed a cost analysis on the turbine itself to determine the economies of scale for designing a specific size (power output) of the turbine. The costs were collected based on previous machining quotes for like machines, material sizing based on ASME Boiler Pressure Codes (for the housing), 1D sizing of the turbine stage, and vendor quotes for bearings, generators, and gearboxes. The costs were compared to the baseline of the NETL (National Energy Technology Laboratory) cost model for sizing (Weiland, Lance, and Pidaparti 2019). Figure 3 shows the economies of scale analyses, which demonstrated there were diminishing returns when moving from a 3MWe turbine to a 5MWe turbine.

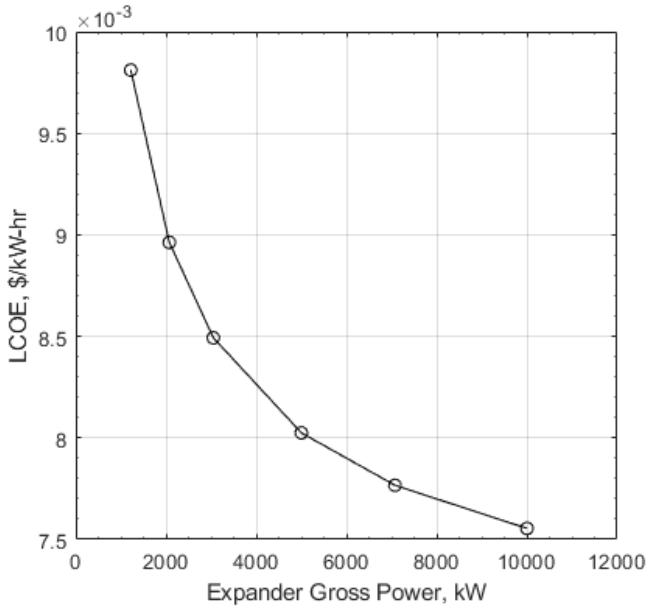

Figure 3. Economies of scale LCOE based on expander output

Finally, a 1D Balje analysis was performed to investigate the optimal RPM for a single stage radial wheel at various power levels (increased flow). Although multiple stage turbines were considered, a single stage turbine allows for greater flexibility (it becomes simpler to switch out the aerodynamic portion), reduces the number of shaft seals (reducing leakage and power loss) and reduces the amount of machining for manufacturing. Figure 4 shows the results with power ranging from 1MWe to 4MWe. As power increases due to higher flows, the optimal rotation speed decreases. Regardless, 22,000 RPM was seen as the option that could meet multiple power levels allowing the turbine to be very flexible.

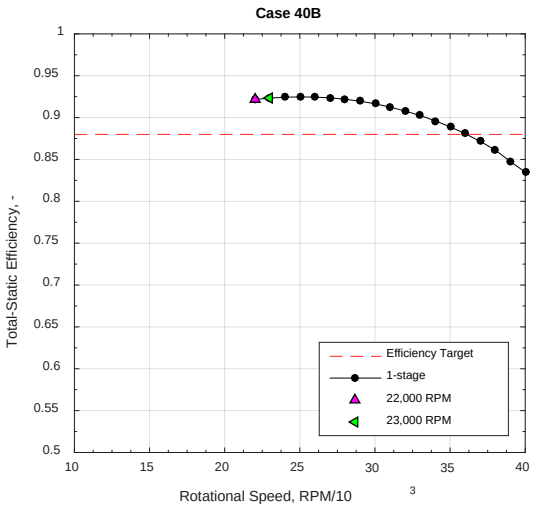
Case 40B
Total-Static Efficiency, -
Rotational Speed, RPM/10^3
Efficiency Target
1-stage
22,000 RPM
23,000 RPM

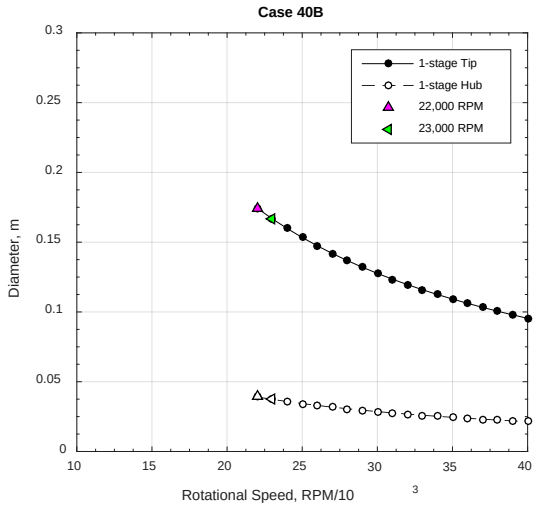
Case 40B
Diameter, m
Rotational Speed, RPM/10^3
1-stage Tip
1-stage Hub
22,000 RPM
23,000 RPM

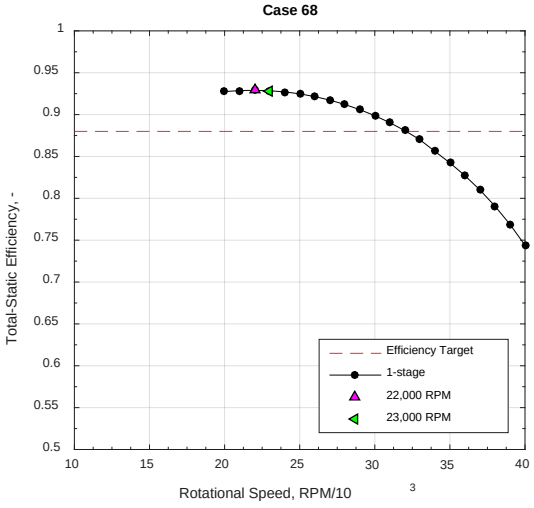
Case 68
Total-Static Efficiency, -
Rotational Speed, RPM/10^3
Efficiency Target
1-stage
22,000 RPM
23,000 RPM

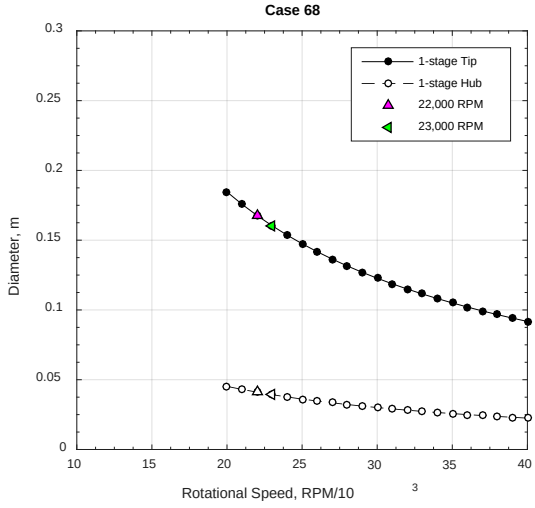
Case 68
Diameter, m
Rotational Speed, RPM/10^3
1-stage Tip
1-stage Hub
22,000 RPM
23,000 RPM

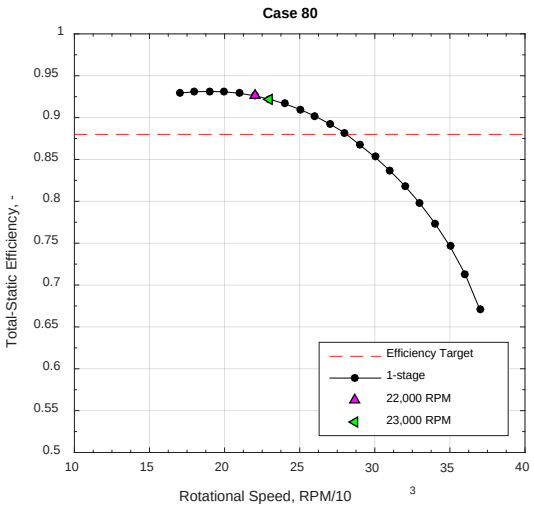
Case 80
Total-Static Efficiency, -
Rotational Speed, RPM/10^3
Efficiency Target
1-stage
22,000 RPM
23,000 RPM

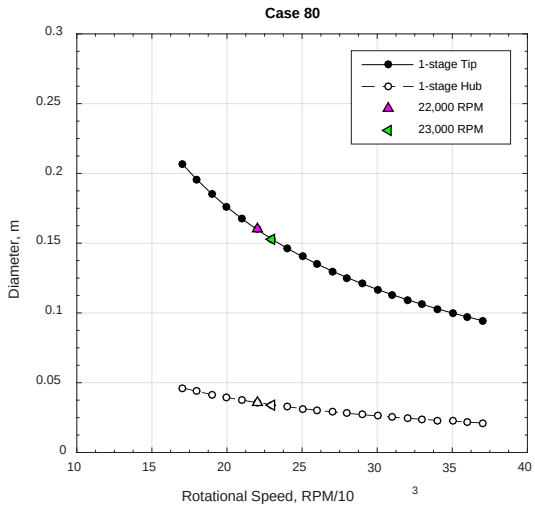
Case 80
Diameter, m
Rotational Speed, RPM/10^3
1-stage Tip
1-stage Hub
22,000 RPM
23,000 RPM

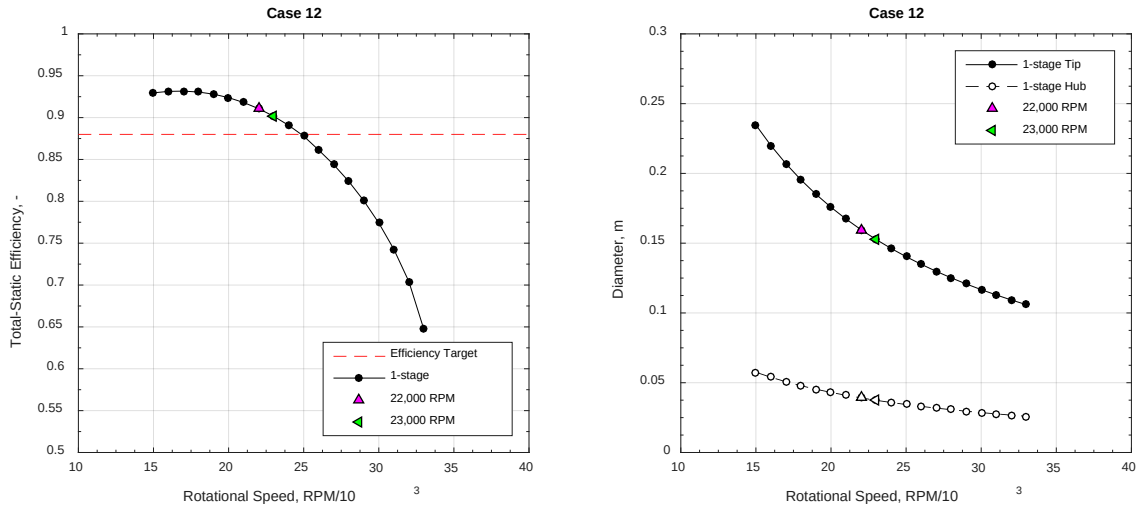

Figure 4. 1D Balje analysis of rotational speed of various power wells (Lowest flow (Case 40), Lower flow(Case 68), Higher Flow (Case 80), Highest Flow (Case 12))

The above analysis is a summary of a more complete analyses performed to determine the operating envelope of the turbine, whose results are shown in Table 1. The maximum power output was based on well operating conditions and the diminishing returns of larger turbines. The inlet pressure was based on the yearly operating conditions and fluctuations examined. These are also based on optimal pressure inlet conditions for a binary plant as well. The inlet pressure was determined by the year-round simulation based on the ambient temperature fluctuations. The rotation speed was selected to cover a wide range of operating power outputs.

Table 1. Turbine Operating Parameters

Condition	**Range**
Power Output	0.5 to 3MWe Output
Operating Speed	22,000 RPM
Inlet Pressure	22.5 MPa max
Outlet Pressure	10 MPa max
Inlet temperature	175°C max

2 Turbine Design

Figure 5 shows the full turbine assembly. The generator has a full 3MWe output and operates at 1800 RPM. It is synchronous and will therefore operate at a constant speed. The gearbox converts the rotational speed of the turbine (22,000 RPM) to the speed of the generator.

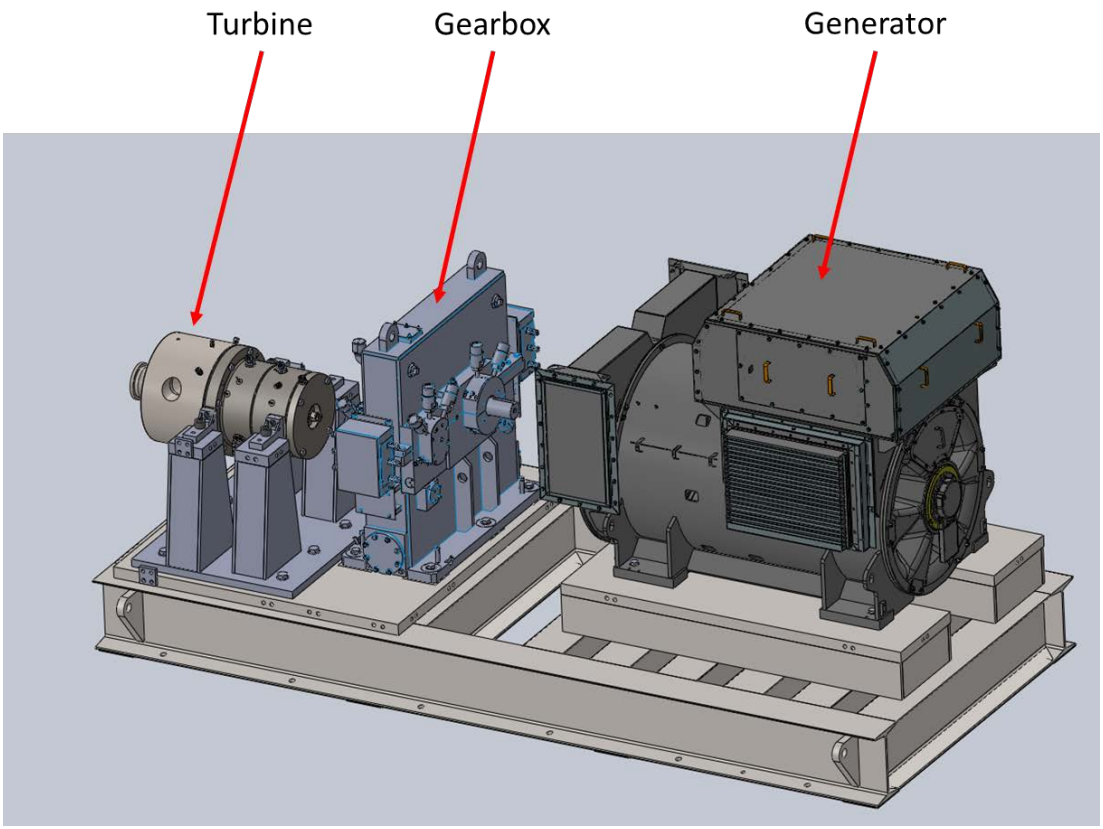

Figure 5. Full Turbine Skid Assembly.

A cutout view of the turbine design is shown in Figure 6. The turbine is a radial wheel with an overhung design. The turbine is supported by oil film bearings such that it's rotor dynamically operates below the first critical speed. Fluid film thrust bearings also accommodate the large thrusts that are possible during off design due to the nature of thrust balance of an overhung turbomachine. The oil is filled and collected in oil housings that will be assembled with the shaft installed.

The turbine is housed in a pressure case that was designed per the ASME (American Association of Mechanical Engineers) boiler and pressure vessel code. Additionally, the turbine is designed such that the aerodynamic portion, which includes the volute, nozzle, and turbine stage, are interchangeable. This allows for flexibility in the following three cases.

First, the different well configurations, as shown in Figure 1 deliver a wide range of turbine inlet conditions possible for different well sites. A flexible aerodynamic design will allow for an optimized design for a range of well conditions.

Second, as the well progresses through its life cycle, it will likely degrade resulting in different operating conditions than originally designed. This will allow the operator to replace the aerodynamic portion of the turbine to a more optimized design as the well conditions change.

Finally, as shown in Figure 2, the nature of sCO2 causes wide variations in density in response to different ambient conditions. This presents some challenges, but one way of overcoming these challenges is to employ different aerodynamic designs at different portions of the year that allow

smaller or larger pressure ratios. The turbine was designed such that the changing of the aerodynamic sections can occur within typical maintenance windows and would not increase the downtime.

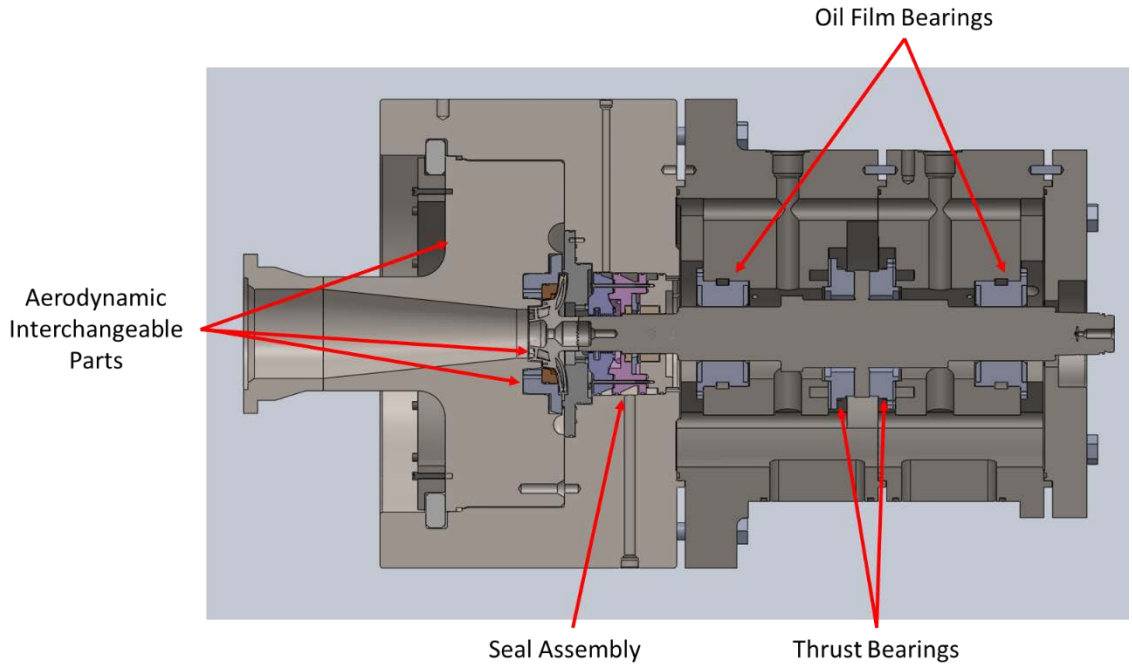

Figure 6. Turbine Design

Finally, one of the major goals of the project is to validate and improve upon the modeling techniques of the aerodynamics of sCO2 turbines to better quantify future plant designs. During the design, the team performed CFD (Computational Fluid Dynamics) to quantify the aerodynamic performance of the turbine stage. The initial CFD was performed for a turbine design that would be tested on the SwRI flow loop, which limits the flow and power output (described in more detail below). These target inlet conditions were 15.75 MPa inlet, 7.5 MPa outlet, 15 kg/s and 150°C. This aerodynamic design, used for bench testing only, is estimated to yield approximately 400-550 kWe power output.

Figure 7 shows the CFD results of the turbine at different flow rates. The current CFD efficiencies do not include seal losses, although current CFD is being performed to quantify those losses. The flow enters the volute, and the velocity is increased through the nozzle. The flow is then converted to rotational energy as the sCO2 continues to expand. The CFD was performed at multiple flow rates to quantify an expected “turn down” or off design conditions. The CFD will be used as a benchmark during testing. Losses of the entire power train will also include losses due to the bearings, gearbox, and generator. Because the test will be at a lower power output than the design, these losses will be a larger portion of the gross power output from the shaft.

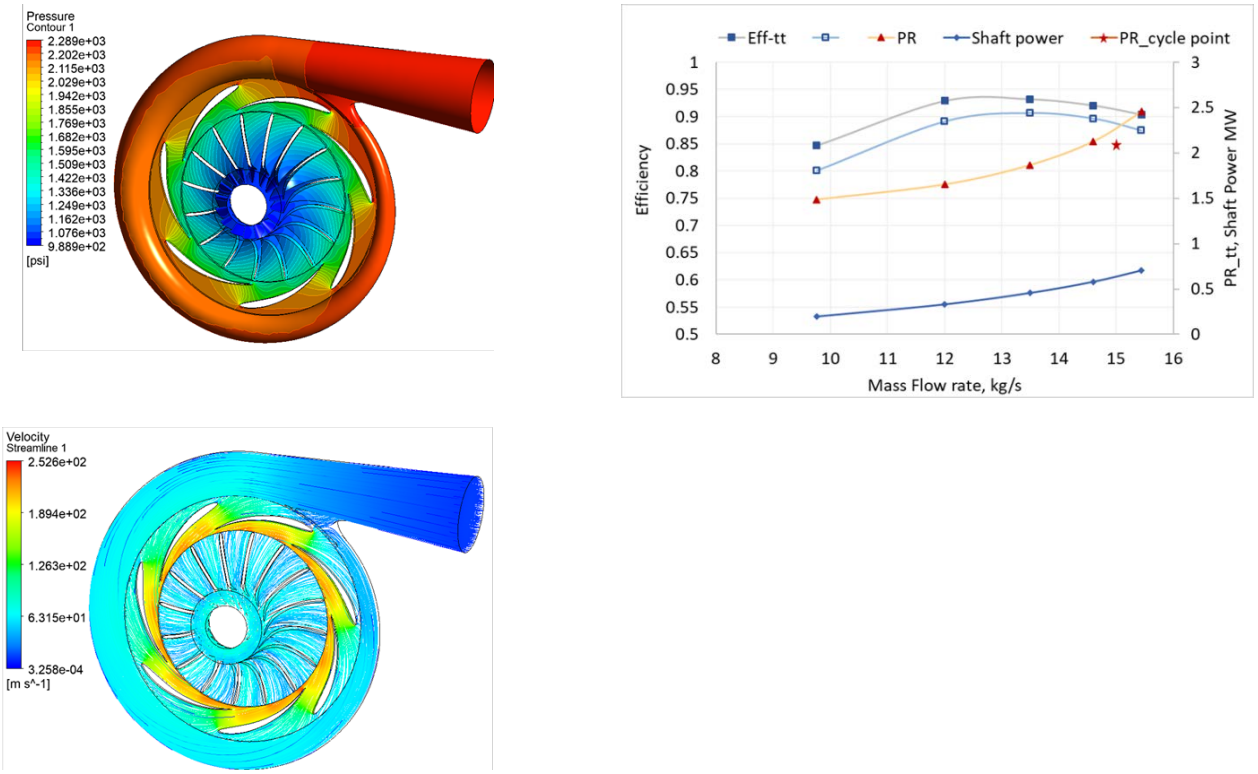

Figure 7. CFD of the aerodynamic design of the test turbine blade.

To maintain the ambitious timeline of a full-scale prototype turbine test by Q3 2022, the team utilized several supply chain and project management skills. First, an initial risk register was performed at the beginning of the detailed design. Table 2 shows the hierarchy of major components for design and procurement. The grading scale is as follows:

Risk Factor: Multiplayer based on prior experience

Cost: 1: <$10k, 2: <$25k, 3: <$75k, 4: <$400k, 5: Other

Lead Time: 1: <5 weeks, 2: <8 weeks, 3: <16 weeks, 4: <25 weeks, 5: Other

The risk register allowed the team to construct a critical path timeline, where long lead items with minimal risk could be placed on order. The result allowed for a bulk of the engineering time to be spent in parallel to kicking off the procurement process. For example, more time was allocated to procuring the gearbox due to its risk ranking (i.e., high) compared to the bearings.

Table 2. Critical Component Risk Register

Item	Risk Factor	Cost	Lead Time	Total
Generator	2	3.5	4	28
Gearbox	2	4	5	40
Forgings	3	2	2	12
Machining	5	2	1	10
Skid	4	2	3	24
Lube Oil System	3	2	3	18
Bearings	3	1	1	3
DAQ	2	1	3	6
Valves	3	2.5	3	22.5

The next skill utilized throughout the process was visual project management. The team quickly adopted an online collaborative project management software that allows for real-time updates to the schedule. Figure 8 shows the inclusion of task dependencies, available slack, and red critical path. Through weekly project management meetings, the team successfully identified new items that impact the critical path that require immediate solutioning. As a result, the team was able react quicker to unexpected and unprecedented global supply chain issues and other potential project delays.

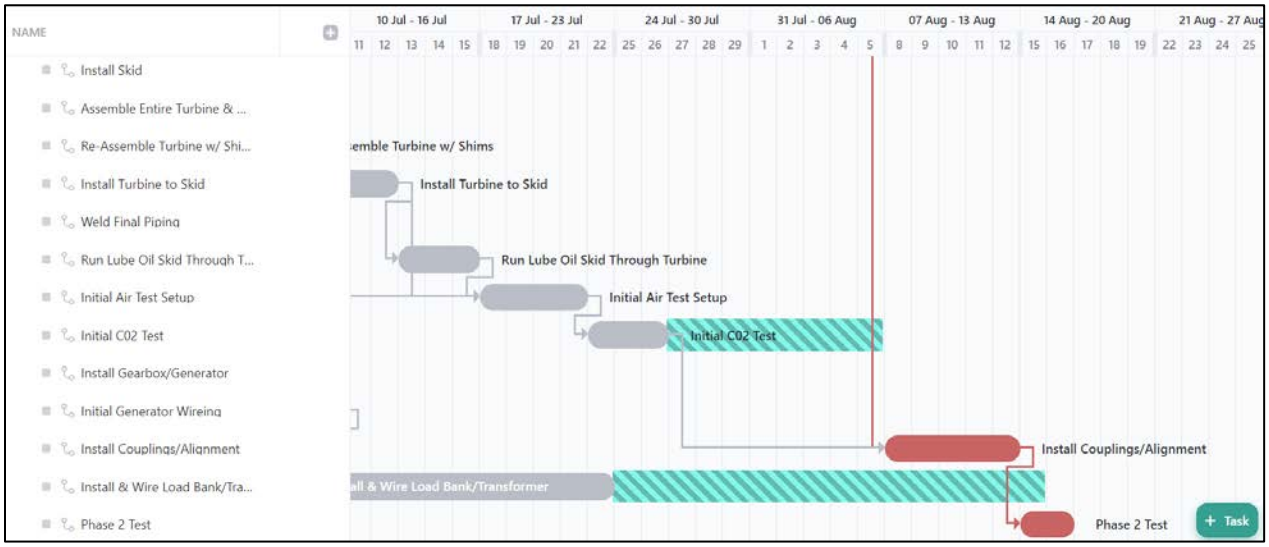

Figure 8. Example Screenshot of online project management software tool

The third skill utilized was to source alternative vendors and procure backup parts for key components. With respect to the intricate turbine casing shown in Figure 6, duplicate forgings were procured to ensure minimal impact to the timeline in the event of scrapping a part during

machining. These redundant parts, in turn, can still be used for future iterations and build outs of the turbine.

3 Turbine Testing

The team will utilize the sCO2 flow loop developed at SwRI to bench test the turbine. The performance of multiple components (e.g., heater, compressor, etc.) in the flow loop were quantified to identify the closest possible conditions to the final sCO2 turbine design that could be replicated in the flow loop testing. The team prioritized matching the pressure ratio, exit turbine pressure, and inlet temperature as close to field conditions as possible. This could be achieved but resulted in a lower flow rate, or approximately 15 kg/s. Therefore, the initial turbine stage was designed to this lower flow rate. Future field applications will require the aerodynamic portion of the sCO2 turbine to be redesigned for higher flow conditions.

The high-level process diagram is shown in Figure 9. A compressor will generate the flow and pressure ratio required to spin the turbine. The flow can go through two paths. The first is a bypass leg that bypasses the turbine completely. During operation the bypass loop will be used to start operating the compressor and allow it to reach the desired operating conditions. Once the desired flow and head are reached, the control valve will be opened to allow flow through the heater, and then through the turbine, where it is expanded down to the suction pressure of the compressor. The flow is combined with any additional bypass flow and continues through a cooler before being compressed.

The goal of the testing is threefold,

1. To validate the mechanical integrity of the entire drive train (i.e., ensure the vibrations fall within specification)
2. To validate the support systems (e.g., lube oil and seal support systems)
3. To measure and verify the aerodynamic performance of the turbine stage (i.e., measure the power generation and compare it to expected results based on operating conditions)

The team will validate the mechanical integrity and support systems by first performing a spin test of the sCO2 turbine using air without the turbine coupled to the gearbox. The air test will provide a low risk test to validate both the lube oil system and the seal support system. These systems will have multiple pressure and temperature sensors to measure that they are functioning as intended/designed. The test will use proximity probes to measure the shaft position at multiple points, specifically next to the bearings. This will validate the rotor dynamic stability of the system. Second, an air test will be performed with the gearbox and generator attached. The team will similarly quantify the vibration data of both the gearbox and generator.

The aerodynamic performance will be measured with a test using CO2 at pressure and temperature. The aerodynamic performance will be measured using the turbine inlet and outlet conditions (pressure and temperature) as well as the flow through the turbine. The flow will be measured with an orifice flow meter. The orifice flow meter is a calibrated orifice that is used to correlate pressure drop to a velocity. The inlet temperature and pressure are used to estimate a fluid density. The fluid velocity and density are combined into a mass flow rate. Although there can be large uncertainty in density measurements of CO2 near the critical point (studies show these can be as high as 10%), the orifice meter is placed on the upstream side where the high

pressure and temperature make sCO2 act close to an ideal gas and the density uncertainty is <1%.

The aerodynamic efficiency is evaluated using Eq. 1 with the static pressures (static to static) comparing the actual enthalpy to the isentropic efficiency. As with the density, the enthalpy is estimated from the pressure and temperature measurements as described by API 617. Additional static measurements will be taken after the nozzles to further validate the CFD model. The power output of the electric generator will be measured such that the team can quantify the total losses from the aerodynamic power to the electric generator.

$\frac{h_{inlet} - h_{exit}}{h_{inlet} - h_{isen}}$	Eq. 1

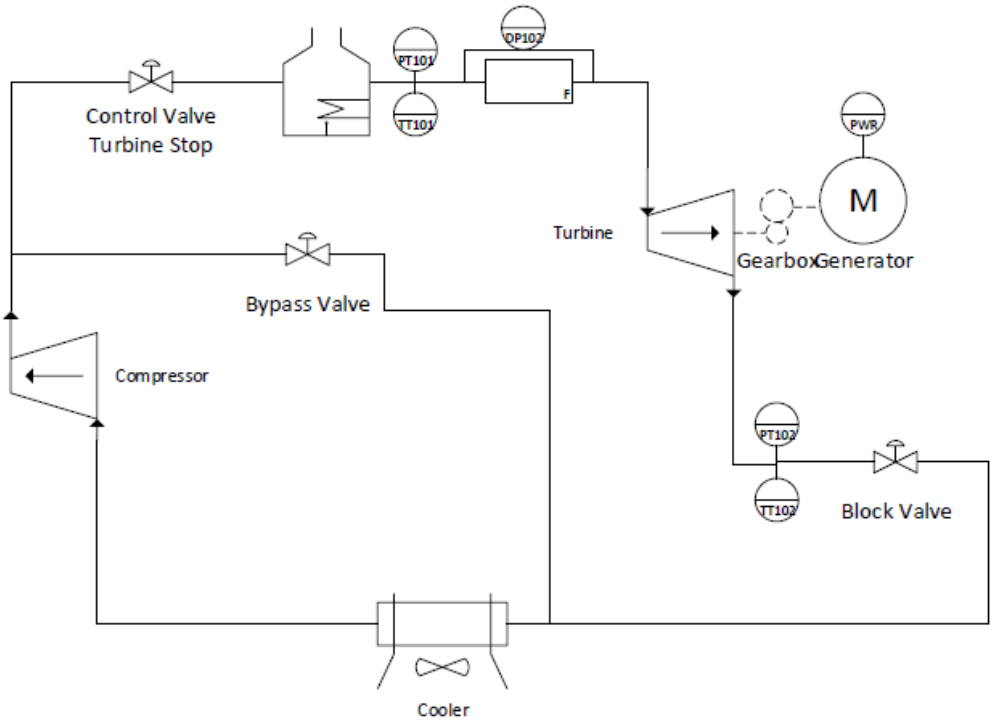

Figure 9. High level process and instrumentation diagram.

Table 2. Instrumentation used for the testing of the turbine

Measurement	PN	Accuracy	Sensor Tags
Pressure	EJA530E-JDS4N-012EL/FF1/D1/N4	0.04% Span	PT-101 PT-102
Differential Pressure	C13ST-2GSET-NN-NN-NNNNN-NNNN/ATCH	0.04% Span	DP-102
Temperature	TMQ316SS-125G-12	1.5	TT-101 TT-102

4 Conclusions and Path Forward

In conclusion, the design and subsequent testing of this proprietary 3MWe sCO2 turbine aligns with Sage's pursuit of mid-enthalpy geothermal. The estimated increase in efficiency in converting heat to electricity, combined with the significant reduction in cost as compared to traditional ORC power plants, will enable mid-enthalpy geothermal to be cost-competitive with wind, solar, and natural gas on an LCOE basis.

Flexibility built into the sCO2 turbine design enables peak performance of the turbine by changing out the aerodynamic components as conditions change over time. In geothermal wells, the key parameters impacted are pressure, flow rates, enthalpy (Aragón-Aguilar, Barragán, and Arellano 2016). Further referenced in our previous techno-economic analysis of a geothermal sCO2 plant, the path to achieving total optimized cost and thermal efficiency is to perform additional sCO2 thermosiphon testing.

REFERENCES

Aragón, A. & Barragán, Rosa & Arellano, V.. (2016). "Analysis of production-decline data: Case of geothermal wells as renewable energy. International Journal of Scientific Research". 6. 2250-3021.

Aragón-Aguilar, Alfonso, Rosa M. Barragán, and Víctor Arellano. 2016. "Analysis of Production-Decline Data: Case of Geothermal Wells as Renewable Energy." *IOSR Journal of Engineering* 6 (10): 32–40.

Atrens, Aleks D., Hal Gurgenci, and Victor Rudolph. 2009. "CO2 Thermosiphon for Competitive Geothermal Power Generation." *Energy & Fuels* 23 (1): 553–57. https://doi.org/10.1021/ef800601z.

De Jesus, A. C. 2016. "Environmental Benefits and Challenges Associated with Geothermal Power Generation." In *Geothermal Power Generation*, 477–98. Elsevier.

Eliasson, Einar Tjörvi, Sverrir Thorhallsson, and Benedikt Steingrímsson. 2011. "Geothermal Power Plants." *Short Course on Geothermal Drilling, Resource Development and Power Plants, Santa Tecla, El Salvador*.

Katcher, Kelsi M., Michael Marshall, Natalie R. Smith, and Cole Replogle. n.d. "ESTIMATED COST AND PERFORMANCE OF A NOVEL SCO2 NATURAL CONVECTION CYCLE FOR LOW-GRADE WASTE HEAT RECOVERY."

Nielson, Jordan, Kelsi Katcher, and Douglas Simkins. 2022. "Techno-Economic Analysis of a Geothermal SCO2 Thermosiphon Power Plant." *The 7th International Supercritical CO2 Power Cycles Symposium*.

Persichilli, Michael, Alex Kacludis, Edward Zdankiewicz, and Timothy Held. 2012. "Supercritical CO2 Power Cycle Developments and Commercialization: Why SCO2 Can Displace Steam Ste." *Power-Gen India & Central Asia* 2012: 19–21.

Sudhoff, Robin, Stefan Glos, Michael Wechsung, Benjamin Adams, and Martin O. Saar. 2019. "Next Level Geothermal Power Generation (NGP)–A New SCO2-Based Geothermal

Concept.” In *German Geothermal Congress/Der Geothermie Kongress (DGK 2019)*, P-25. ETH Zurich.

Weiland, Nathan T., Blake W. Lance, and Sandeep R. Pidaparti. 2019. “SCO2 Power Cycle Component Cost Correlations From DOE Data Spanning Multiple Scales and Applications.” In . American Society of Mechanical Engineers Digital Collection. https://doi.org/10.1115/GT2019-90493.